



EFFECT OF SPACER THICKNESS ON THE OVERALL ENERGY CONSUMPTION OF BPMED USING AMMONIUM SULFATE SOLUTION

HITESHREE MITHAIWALA

Student no.: 5564131

Ph.D. supervisor: Ir. Dhavissen Narayen

Professors: Dr. Ir. Henri Spanjers, Prof. Dr. Ir. Jules Van Lier



Abstract

Removal of ammonium from simulated ammonium salt solutions was done using bipolar membrane electrodialysis (BPMED), without the use of chemicals. The effect of spacer thickness and open area on the overall energy consumption of BPMED to transport ammonium from the diluate was assessed in batch experiments. The electrochemical energy consumption decreased from 28 MJ/Kg-NH₄⁺ to 16 MJ/Kg-NH₄⁺ when the spacer thickness decreased from 750 μm to 140 μm.

The removal efficiencies of ammonium from the diluate increased from 77% to 85% when the spacer thickness decreased from 750 μm to 140 μm. These results show that with the increasing spacer thickness, the open area and porosity also increase, which accounts for higher resistance on the membrane stack. However, besides open area and porosity, it is the thickness of the spacer that plays a major role in higher energy consumption. This study demonstrated the energy-efficient application of BPMED for the removal of ammonium from simulated ammonium salt solutions.

Contents

1. Introduction:	4
1.1 Removal of ammonium from wastewater	4
1.2 Bipolar Membrane Electrodialysis for removal of ammonium from residual waters.....	4
1.3 About Spacers in BPMED	4
1.4 Problem Description and research objective	5
2. Materials and Methods:.....	6
2.1 Materials	6
2.2 Methods	7
2.4 Performance indicators for calculating the mass of NH_4^+ in all the compartments.....	8
2.4.1 Computation of Open area of spacers	8
2.4.2 Computation of Porosity of spacers.....	8
2.4.3 Computation of electrochemical energy.....	9
3. Results and Discussion:	10
3.1 Evaluation of BPMED's spacers' open area and porosity	10
3.2 Removal of ammonium from diluate to acid and base.....	10
3.2.1 Evaluation of Diluate	11
3.2.1.1 Comparison between different spacers for efficient removal of ammonium from diluate into acid and base	12
3.2.2 Evaluation of Base	13
3.2.3 Evaluation of Acid.....	13
3.3 Diffusion of NH_3 through the BPMED membrane stack.....	14
3.4 Assessment of electrochemical energy consumption.....	14
4. Conclusion:.....	16
5. References:.....	17
6. Supplementary Index:	19
SI.1 Experimental Set-up	19
SI.2 Microscopic views of different spacers (with different thickness) along with measurements	21
SI.2.1 140 μm thick spacer:	22
SI.2.2 450 μm thick spacer:	23
SI.2.3 750 μm thick spacer:	24
SI.3 pH and EC graphs for all the compartments	25
SI.3.1 Diluate	25

SI.3.2 Base	26
SI.3.3 Acid.....	27
SI.4 Values and graphs of ammonium and sulfate concentrations throughout the batch	28
SI.4.1 Ammonium conc.:	28
SI.4.2 Sulfate Conc.:.....	30
SI.5 Computation of average electrochemical energies for other data	32

1. Introduction:

1.1 Removal of ammonium from wastewater

In this study, it is important to look at NH_4^+ which is normally the case for residual wastewater which contains a high amount of ammonium ions. From the study of (Mehta et al., 2015), it was observed that struvite precipitation and air stripping along with acid scrubbing can remove high concentrations of nitrogen as fertilizer from residual wastewater. But these processes have many disadvantages such as it involves huge amount of use of chemicals (which needs proper care and attention), it also needs cost of operation etc.

However, to restrict the use of chemicals and just using energy for removal of ammonia, Kuntke et al., (2018); Xie et al., (2016) studied that electrodialysis can be widely used as it does not use any chemicals.

1.2 Bipolar Membrane Electrodialysis for removal of ammonium from residual waters

Bipolar membrane electrodialysis is the separation of anions and cations by applying electrical energy, in which the anions and cations react with protons (H^+) and hydroxide ions (OH^-) respectively, produced by the splitting of water molecules by the bipolar membranes (BPMs) (van Linden et al., 2020). This results in an acid and a base solution.

Recently, the study by (van Linden et al., 2020) tested BPMED for ammonium removal, where the TAN removal efficiency ranged between 85-91% and the concentration of ammonia in the base was noted to increase from 1.5 to 7.3 g/l. Moreover, Kuntke et al. (2018) noted that the BPMED works on energy consumption with 85-90% removal of nitrogen concentrations. Whereas other methods of nitrogen removal (such as anammox and air stripping) works on use of chemicals in water treatment. Thus, BPMED proved to have no waste products and is environmentally friendly (Zheng et al., 2022).

1.3 About Spacers in BPMED

Spacers are used in BPMED to maintain distance between membranes and to support ion distribution in solution compartments due to their mesh grid. Previously, different aspects of the spacers such as geometry of spacers, which includes filaments thickness, distance, and angles have been studied to process performance parameters such as pressure drop and mass transfer (Mehdizadeh et al., 2019). With the help of these measurements, it is possible to get the open area and porosity of spacer. The calculations for open area and porosity can be found under section 2.4.1 (Computation of open area of spacers) and 2.4.2 (Computation of porosity of spacers).

The percentage of gaps or unfilled spaces in a spacer material is referred to as porosity. It is a measure of how much space there is inside the spacer for fluid to pass through (Siddiqui et al., 2017). It was observed that with the greater thickness (and larger open area), the porosity also increased (Mehdizadeh et al., 2019). The correlation between spacer geometry (like open area) and porosity has been thoroughly investigated to know the optimum thickness of the spacer

through the use of spacer geometries such as filament diameter, distance, and angle (Mehdizadeh et al., 2019).

1.4 Problem Description and research objective

The resistance of the solution compartment increases as the spacer thickness increases. To reduce power output or overall energy consumption, reduce resistance by taking into account the porosity, thickness and open area on the overall membrane stack (Mehdizadeh et al., 2019; Post et al., 2008). The increase of open area and porosity leads to increasing passage for ammonium ions to pass (Mehdizadeh et al., 2019; Post et al., 2008). However, it is unsure whether increasing thickness, open area and porosity together also increases the electrochemical energy consumption of the BPMED stack.

The objective of the study is to investigate the effect of different spacer thicknesses along with open area and porosity on energy consumption for the removal of ammonium from ammonium sulfate residual effluents.

2. Materials and Methods:

2.1 Materials

We used the BPMED setup, which is a three-compartment setup. This means, Anion exchange membranes (AEM), Cation exchange membranes (CEM), and Bipolar membranes (BPM) are in repeating units to get two produced solutions (i.e., acid and base). The cell contained 10 cell triplets, together adding up to a BPMED membrane stack. Each cell contained one AEM, one CEM, and one BPM as shown in figure 1. Anion Exchange End Membranes (AEEMs) were used to prevent ammonium transport to the ERS. The rest of the BPMED stack contained ten CEMs, nine AEMs, and ten BPMs. The membranes were split up by spacers to form diluate (between AEM and CEM), acid (between BPM and AEM), and base (between CEM and BPM) compartments. For this study, different spacers thicknesses were used, which are 140 μm , 450 μm and 750 μm . All membrane and spacer materials were purchased from PCCell (Heusweiler, Germany).

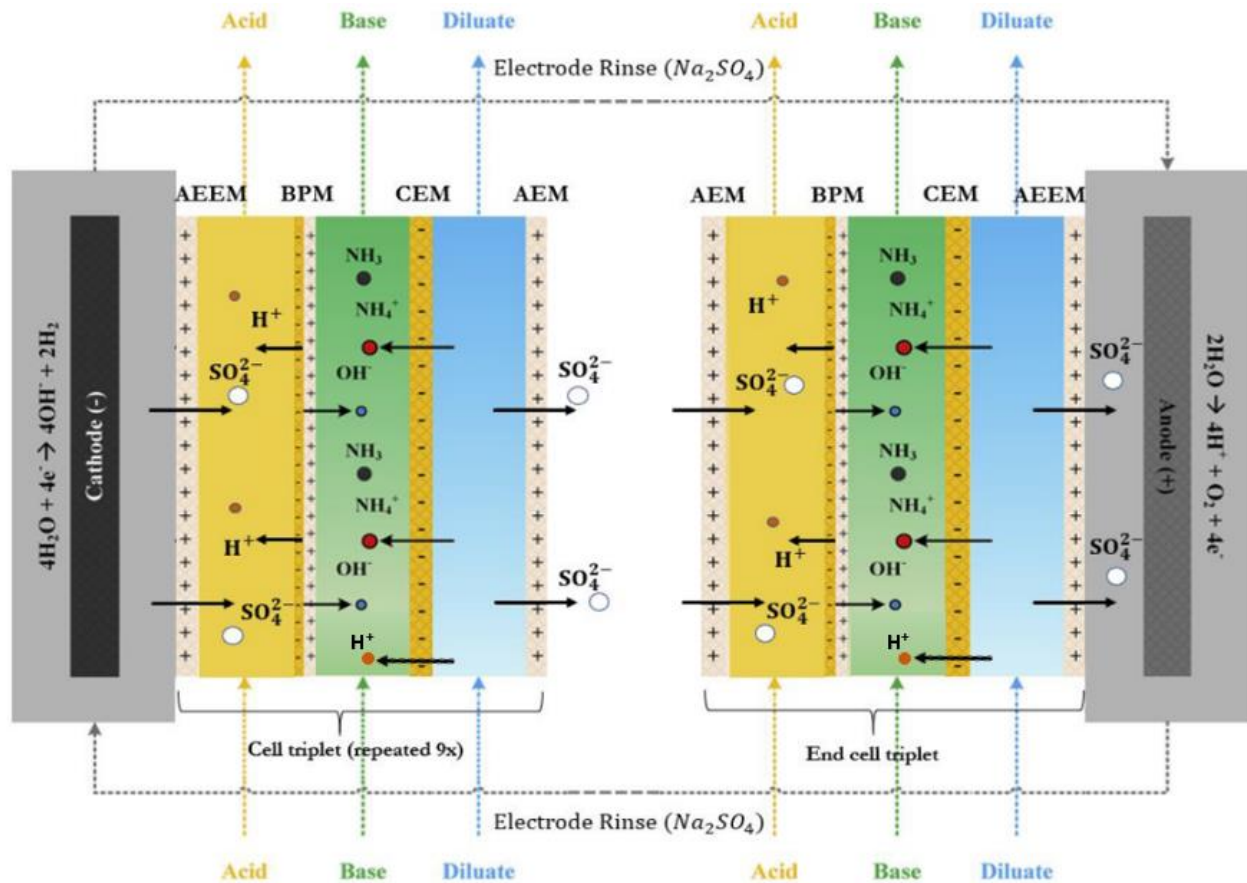


Figure 1: The Bi-polar membrane electro dialysis (BPMED) diagram and the mechanism of ion transfer between the feed and the Acid/Base compartments (van Linden et al., 2020)

Initially, the diluate contained 50 g ammonium sulfate salt ($(\text{NH}_4)_2\text{SO}_4$) ($\geq 99\%$) in 1-liter demi water (corresponding to an ammonium concentration of 13.6 g/l). The acid and base contained 0.66 g ammonium sulfate salt ($(\text{NH}_4)_2\text{SO}_4$) ($\geq 99\%$) in 0.5-liter demi water (corresponding to an ammonium concentration of 0.18 g in 0.5 l). The Electrode Rinse Solution (ERS) contained 71 g

sodium sulfate salt (Na_2SO_4) ($\geq 99\%$) in 0.5-liter demi water. All the reagents were supplied by Sigma Aldrich (Zwijndrecht, The Netherlands). The diluate, acid, base, and ERS solutions were stored in borosilicate bottles, which were constantly stirred with the help of magnetic stirrers on a mixing plate. The solutions from each bottle (diluate, acid, base, and ERS) are pumped in the BPMED membrane stack using a Peristaltic Watson-Marlow 520S pump with separate Watson-Marlow 313 pump heads. The pump was set to a constant flow rate of 16.9 l/hour for the diluate, acid, and base cells. The electric current and potential were applied using a TENMA 72-1330 power supply box. To analyze the pH and EC of the compartments, there were calibrated multimeters for each compartment. For pH, IDS SenTix 940 pH meters and WTW Multi 3620 IDS multimeters, and for EC, TetraCon 925 EC meters and WTW Multi 3620 IDS multimeters. The complete experimental setup is shown in figure 2.

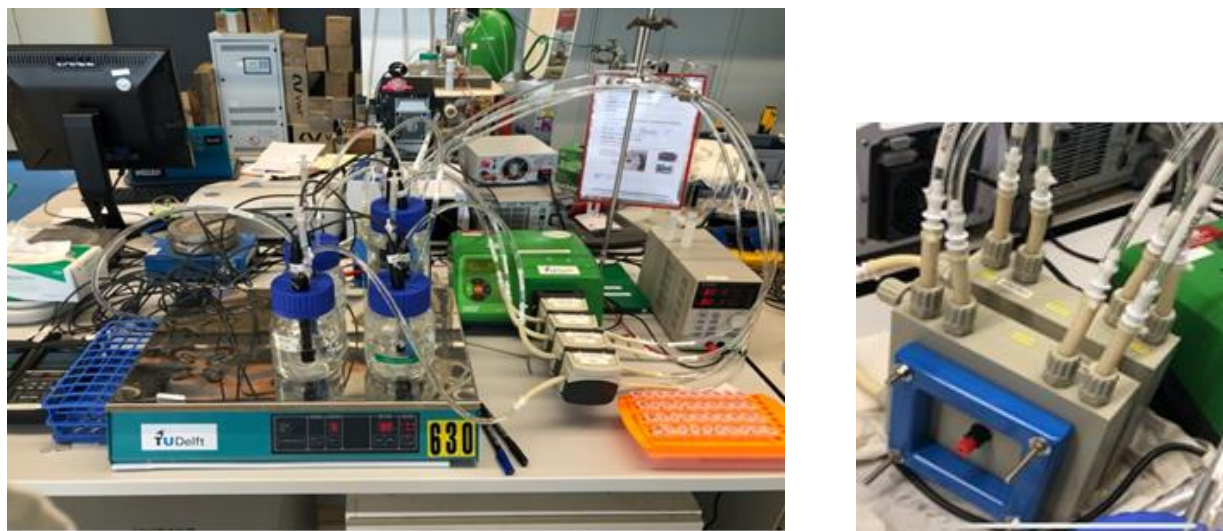


Figure 2: Left image shows the entire experimental setup for the BPMED membrane stack and the right image shows the BPMED membrane stack along with the anode and cathode ports on the sides for electrical energy to pass through it.

All the individual images of the pump, pump heads, power supply box, multimeters (for pH and EC), and solution bottles can be found in the Supplementary Index (SI.1).

2.2 Methods

Batch experiments, to investigate the effect of the spacer thickness and open area of a pore, were performed by using the experimental set-up as shown in Fig.2. In this case, to know the performance of one spacer, triplicates were carried out. For every batch, new diluate, acid, and base solutions were prepared, whereas, for ERS, it was reused. The initial pH of diluate and ERS was adjusted to 4 and 2 respectively with the help of sulfuric acid (2.5 M). The experimental run time was kept for at least 2.5 hours (150 mins). Samples were taken every 15 minutes along with pH and EC sensors at every 5 seconds. Furthermore, pH and EC were constantly recorded with the help of multimeters to check the performance of compartments throughout the cycle.

Solution volumes, mass, pH, and EC were measured manually at the beginning and at the end. The electric current and voltage were constantly logged in the computer to assess the electrochemical energy consumption with the help of a power supply. Once the samples are taken and diluted (by calculating dilution factor) with ultra-pure water, the concentrations of ammonium(cation), sodium(cation), and sulfate(anion) in each compartment can be known with the help of an Ion Chromatography (IC).

2.4 Performance indicators for calculating the mass of NH_4^+ in all the compartments

2.4.1 Computation of Open area of spacers

To calculate the open area of a pore, it is important to know different measurements of pores (such as length, width, angle, etc.) of each spacer as shown in fig.3 (See SI.2). The formula for calculating open area is:

$$\text{Open area} = \frac{L^2}{(L+D_L)^2} \text{ Here, } L, D_L \text{ can be seen from fig. 3 (Post et al., 2008)}$$

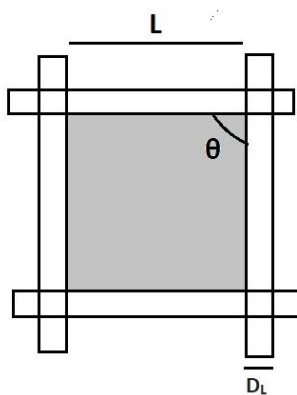


Figure 3: Schematic representation of spacer's pore for geometry calculation where L = mesh opening (mm), D_L = wire diameter (mm), and the shaded portion is the open area of a pore.

2.4.2 Computation of Porosity of spacers

To calculate porosity, there are certain specific parameters which should be known, that are:

- The specific gravity of the material that is used for spacer
- Weight of fabric
- Area of spacer

It is important to note that the material used for all three types of spacers was different as mentioned in the manual by the manufacturer: PC Cell. 140 μm has a combination of 50% Polyester and 50% Silicon; 450 μm thick spacers has a combination of 50% Polypropylene (PP) and 50% Silicon; and 750 μm has a combination of 50% Polyethylene Terephthalate (PET) and 50% Silicon. This corresponds to different specific gravities for all three spacers, which can be seen in the table 1 below.

Table 1: Calculation of specific gravities

Material	Units	Specific Gravity (SG)	Source of SG	140 μm	450 μm	750 μm
Silicon	Kg/m ³	2330	(Wikipedia, 2 September 2023)			
Polyester	Kg/m ³	1390	(Cameo, 4 August 2022)	1860	-	-
PP	Kg/m ³	910	(Pashkevich et al., 2019)	-	1620	-
PET	Kg/m ³	1380	(Cameo, 4 August 2022)	-	-	1855

The formula to calculate porosity can be found in the table 2 below: (from Post et al., 2008)

Table 2: Calculation to measure porosity of a spacer

Parameters	Symbol	Units	Formula
Specific gravity (PET)	SG	Kg/m ³	(from Table 1)
Weight of fabric of 1 spacer	w ₁	Kg	(Manually in laboratory)
Area of 1 spacer	a _t	m ²	(Manually in laboratory)
Weight of total fabric	w _t	Kg/m ²	w ₁ /a _t
App. Gravity	AG	Kg/m ³	w _t /t _{sp}
Porosity	%	-	(1-(AG/SG)) *100

2.4.3 Computation of electrochemical energy

From (van Linden et al., 2020) study, it was determined that with the help of NH₄⁺ mass that went from diluate to base and acid by BPMED and power consumed during the whole experiment, an electrochemical energy consumption equation was built as shown below.

$$E_e = \frac{\sum_{t=0}^t (U_{\Delta t} \cdot I_{\Delta t} \cdot \Delta t)}{m_{\text{NH}_4^+,d}}$$

Here, E_e = electrochemical energy in J g/NH₄⁺, U_{Δt} · I_{Δt} = Power during each time interval in W, Δt = time interval in secs and m_{NH₄⁺,d} = amount of ammonium that was transferred from diluate in g-NH₄⁺.

3. Results and Discussion:

3.1 Evaluation of BPMED's spacers' open area and porosity

With the help of these measurements, the open area of a pore is obtained by taking the average of triplicates, which is 34.3%, 48%, and 46% for 140 μm , 450 μm , and 750 μm thick spacers respectively. These results are similar with different studies (Post et al., 2008; Vermaas et al., 2014) from which we know that different open area with different thickness affects the overall membrane stack's resistance. The thinner the thickness of spacer, the smaller is the pore and thus, the smaller is the resistance it offers on the membrane stack. However, it can be observed that the results are not entirely in line with each other that is because manufacturers of spacers are not particularly making spacers for the BPMED; so, sometimes manufacturers increase the wire density of netting to make the netting strong and this in turn makes the spacer great for the use. Also, there are some random spacers in the stack sometimes which can also change the overall open area and thus, changes electrical resistance, which can be found similar in a catalog from the manufacturer Sefar. The catalog has many different open area and different thickness.



For porosity, the values obtained were 63.5% for 140 μm , 67.8% for 450 μm , and 65% for 750 μm thick spacers. The values of all three spacers have almost negligible difference between each other.

We evaluate different parameters of different spacers' thicknesses under the microscope with high magnification to get better optical views and measurements. The images of three different spacers (with different thicknesses of 140 μm , 450 μm , and 750 μm) can be seen in figure 4.

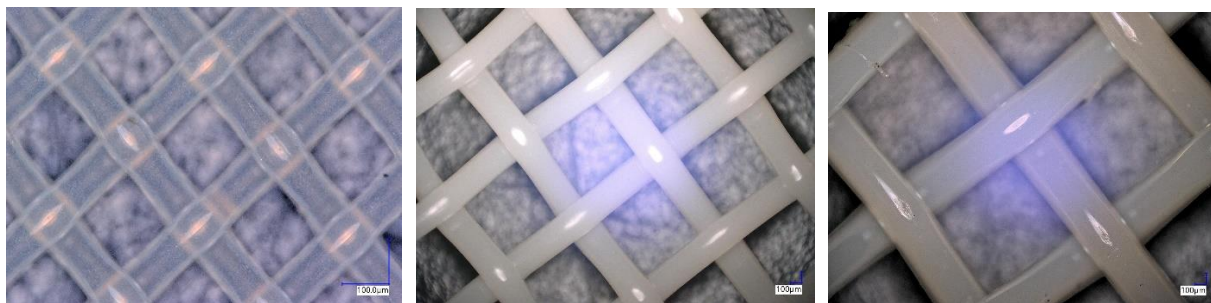


Figure 4: Microscopic views of three types of spacers. The left image is of 140 μm thick spacer, middle image is of 450 μm thick spacer and the third image is of 750 μm thick spacer

3.2 Removal of ammonium from diluate to acid and base

The ammonium removal from diluate transported to acid and base represent the average values calculated from duplicated batches. The table of different values and graphs for ammonium and sulfate can be found in SI.4. The values obtained have a percentage error check of less than 5%.

3.2.1 Evaluation of Diluate

The initial concentration of ammonium in the diluate was about 13.485 g/L. The final concentration were 2.0 g/L, 2.4 g/L, and 3.0 g/L for 140 μm, 450 μm, and 750 μm spacers respectively. This corresponds to the removal efficiencies of 85%, 81.5% and 77%, respectively. The decrease in diluate EC from 61.5 mS/cm to 14 mS/cm, 16 mS/cm, and 19 mS/cm for 140 μm, 450 μm, and 750 μm spacers respectively (as seen in SI.3.1) was observed as the result of efficient ammonium removal from the diluate to the acid and base. As can be seen from the figure below, the thinnest spacer (140 μm) had the lowest EC, which also corresponds to the highest removal of ammonium from the diluate compared to 450 μm and 750 μm EC.

The pH initially in the diluate was 4 and the final pH resulted to approx. 2.3 for all the different types of spacers (as seen in SI.3.1).

The mass percentage in terms of ammonium removal from diluate transported into acid and base is shown in the figure 5 using the below-mentioned formula:

$$M_c(\%) = \left(\frac{M_{c,NH4+}(t = 150 \text{ min})}{M_{D,NH4+}(t = 0 \text{ min})} \right) * 100$$

Where, M_c = Mass compartment (diluate, acid and base) in %,

$M_{c, NH4+}$ = Concentration of ammonium in the compartment at $t = 150 \text{ min}$ (in ppm/l),

$M_{D, NH4+}$ = Concentration of ammonium in the diluate at $t = 0 \text{ min}$ (in ppm/l)

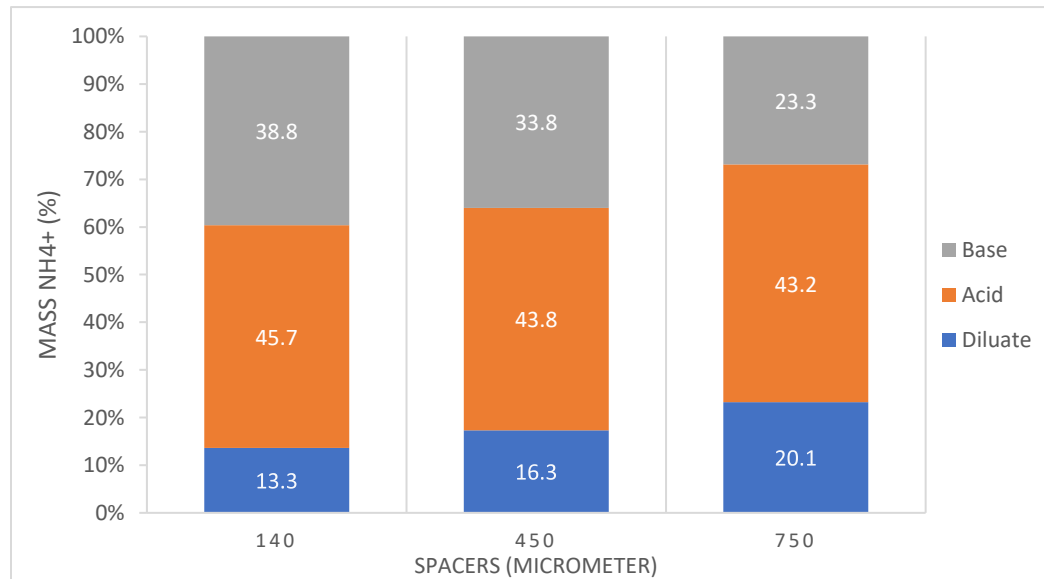


Figure 5: Mass of ammonium transported from diluate to acid and base in terms of percentage

3.2.1.1 Comparison between different spacers for efficient removal of ammonium from diluate into acid and base

As seen from the figure 6, a 140 μm spacer has the best ammonium removal efficiency, followed by 450 μm and 750 μm respectively. This happened probably because 140 μm has the lowest open area available for ions to pass which indicates that it offers the smallest resistance to the whole membrane stack. The porosity of 140 μm is also the smallest as seen previously in the section 3.1 Evaluation of BPMED's spacers' open area and porosity.

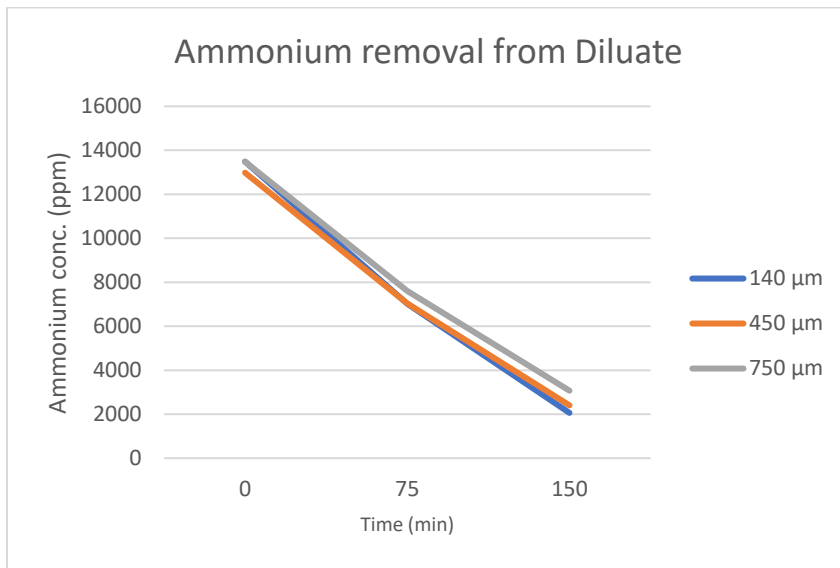


Figure 6: Ammonium removal efficiency from diluate throughout the cycle

140 μm thick spacer seems to be the optimum spacer due to the smallest open area and highest removal of ammonium but it is not the case as can be observed in figure 7, that it offers the lowest resistance, there is easily more diffusion of ammonia through BPMs to the acid.

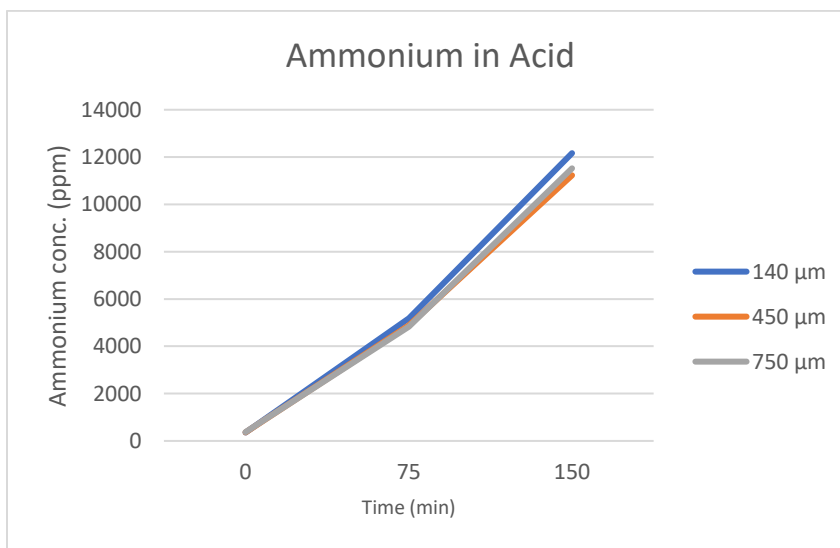


Figure 7: Ammonium accumulation in the acid throughout the cycle

When looking at ammonium in the base (fig. 8), as the spacer thickness increases, the open area of a pore increases, and thus, less amount of ammonia ends up in the base.

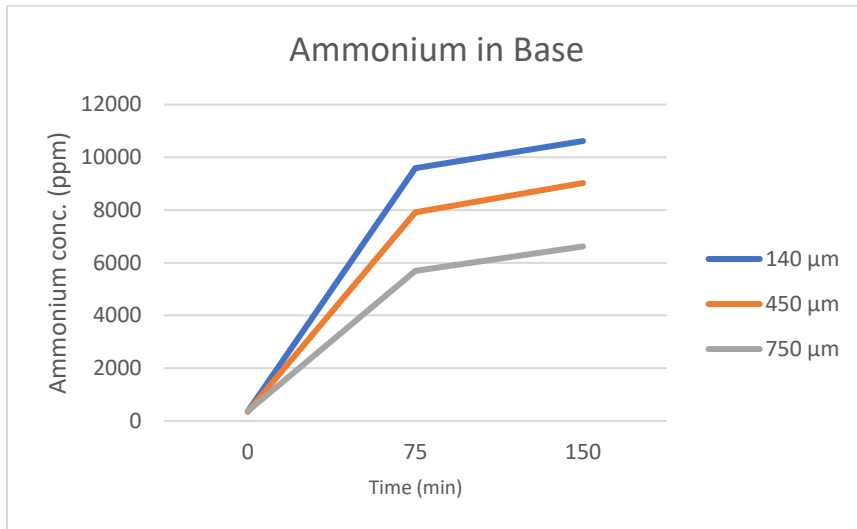


Figure 8: Ammonium accumulation in the base throughout the cycle

The thinner the spacer, the smaller the open area and porosity, which means smaller the resistance (with respect to the thicker spacers), thus, more is the easy transport of ions from the diluate to the acid (diffusion of NH_3) and base.

3.2.2 Evaluation of Base

The initial concentration in the base was about 0.4 g/L to the final concentration of 10.6 g/L, 9.0 g/L, and 6.6 g/L for 140 μm, 450 μm, and 750 μm spacers respectively. The increase in base EC was observed from 2.5 mS/cm to 4.2 mS/cm, 4.1 mS/cm, and 3.9 mS/cm for 140 μm, 450 μm, and 750 μm spacers respectively (as seen in SI.3.2). This proves that there was systematic transport of ammonium in the base from the diluate. The thinner the spacer, the better ammonium ion is transported in the base.

The base pH reached a steady state at 10.7 (as shown in SI.3.2) for all three types of spacers but as seen in previous studies (Li et al., 2016; Shi et al., 2018), the values reached higher than 11. The reason for this could be due to the consumption of hydroxide ions by ammonium, which gave product of ammonia and water. This is because a portion of the OH^- produced by the BPMs did not result in a rise in base pH.

3.2.3 Evaluation of Acid

The initial concentration in the acid was about 0.4 g/L to the final concentration of 12.2 g/L, 11.2 g/L, and 11.5 g/L for 140 μm, 450 μm, and 750 μm spacers respectively. The acid EC was seen increasing from 2.5 mS/cm to 109 mS/cm, 105 mS/cm, and 94.8 mS/cm for 140 μm, 450 μm, and 750 μm spacers respectively (as seen in SI.3.3). This means that there was a lot of back diffusion of ammonium from the base. 140 μm spacer has the highest ammonium concentration when compared to the other two spacers.

As the ammonia concentration slope between the base and acid increased with all the SBEs, the ammonia diffusion to the acid also increased. The diffused NH_3 acted with H^+ in the acid, resulting in a sharp rise in acid EC.

The acid pH increased to up to 1.1, 1.0, and 1.1 for 140 μm , 450 μm , and 750 μm spacers respectively (SI.3.3). This increase is due to NH_3 diffusion and hydroxide ions (OH^-) leakage from the base.

3.3 Diffusion of NH_3 through the BPMED membrane stack

In the previous study (van Linden et al., 2020), it is shown that the NH_3 concentration in the acid increased from 0 to 3.1 g/L. That is due to the diffusion of NH_3 that took place through BPMs to the acid. The NH_3 concentration variation between the base and acid decreased over time due to a decrease in NH_3 concentration in the base. The concentration of NH_3 in the acid was consistently higher than in the diluate, indicating that NH_3 escaped effortlessly from the base to the acid via the BPMs than from the base to the diluate via the CEMs.

3.4 Assessment of electrochemical energy consumption

As can be seen from the figure 9, the higher electrochemical energy is consumed/required for the transportation of ammonium from the diluate when 750 μm thick spacers were used. This higher energy with thicker spacers accounts for higher resistance that was encountered when transporting ammonium ions from diluate. The higher energy consumption is also due to the low current efficiency of ammonium ions as was previously discussed by (van Linden et al., 2020) in his study. Thus, the decline in the electric potential was caused by an increase in acid EC and base EC through the run, which overall resulted in a decrease in the BPMED membrane stack's electrical resistance which can be seen for the case of 140 μm and 450 μm thick spacers. Whereas for 750 μm thick spacer, we observe a higher energy consumption (28.4 MJ/Kg- NH_4^+) which is due to larger electrical resistance.

From previous studies (Post et al., 2008; Vermaas et al., 2014), we understood that porosity, open area and thickness all together make up to the resistance of membrane stack. The amount of membrane resistance gives us the electrochemical energy required to transport the ammonia from the diluate. We also understood from the section 3.1 (Evaluation of BPMED's spacers' open area and porosity) that open area and porosity of all the three spacers have almost negligible difference between them and thus, does not count as a major factor in variation of energy requirement. So, here in electrochemical energy evaluation, thickness plays a major role as observed from the fig. 9 below. Therefore, 750 μm being the thickest spacer among all three spacers requires the highest electrochemical energy consumption (28.4 MJ/Kg- NH_4^+) and 140 μm being the thinnest spacer accounts for lowest energy consumption (16.2 MJ/Kg- NH_4^+) among three spacers.

Note: For the computation of electrochemical energy, it is important to mention that the current was kept constant at 1.2 A throughout the operation of the BPMED. The average initial electric potential was kept at 30 V initially for 140 μm and 450 μm . However, for 750 μm , it was observed

that there was larger resistance to the membrane stack (due to the thickness of the spacer and also, due to more open area) as the voltage was not varying and the current started dropping. So, the potential was increased to 45 V for a 750 μm spacer. Therefore, throughout the batches, the electric potential was observed and was noted at 16 V, 18.5 V, and 26 V for 140 μm , 450 μm , and 750 μm spacers, respectively at the end of the batches.

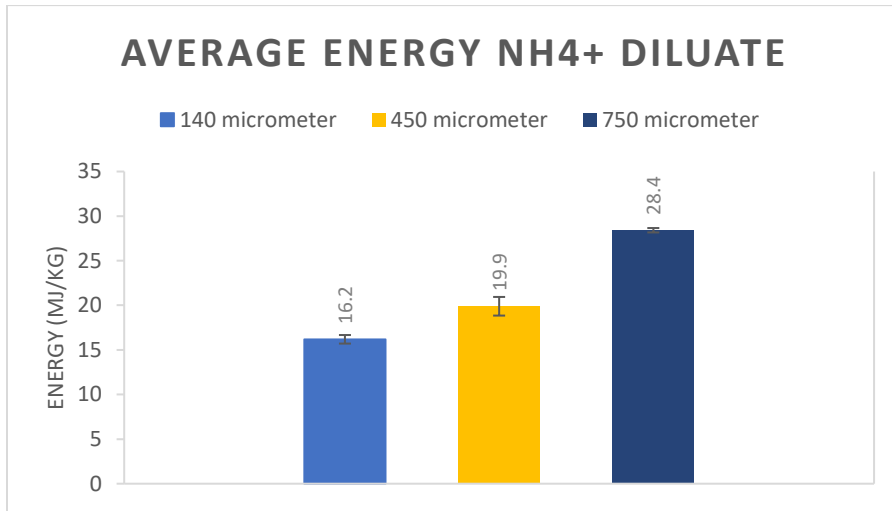


Figure 9: Comparison between different spacers on the average energy consumption to transport ammonium ions from diluate

The different values and graphs for other electrochemical energy which can be compared to the average energy consumption for ammonium removal from diluate can be found in the Supplementary Index (SI.5).

4. Conclusion:

BP MED with different spacer thicknesses proved that with increasing thickness and the increasing open area and porosity of spacers, the resistance on the overall membrane stack increases. Ammonium ions from the diluate were transported most efficiently by the thinnest spacer (140 μm) followed by thicker spacers as the removal efficiency for ammonia from diluate for 140 μm thick spacer was observed 85%, for 450 μm was 81.5% and for 750 μm was 77%.

Lower electrochemical energy consumption was observed for thinner spacers than thicker spacers. The average energy obtained for ammonium removal from diluate using ammonium sulfate solution was 16 MJ/Kg-NH₄⁺ for 140 μm thick spacer, 19 MJ/Kg-NH₄⁺ for 450 μm thick spacer, and 28 MJ/Kg-NH₄⁺ for 750 μm thick spacer.

However, it was observed that with the thinnest spacers (with the smallest open area and porosity), large diffusion of ammonium through the BPMs to the acid compartment was obtained. This allows NH₃ to escape easily from the base to the acid.

5. References:

- Cameo. (4 August 2022). Retrieved from https://cameo.mfa.org/wiki/Polyester_fiber
- Kuntke, P., Sleutels, T. H. J. A., Rodríguez Arredondo, M., Georg, S., Barbosa, S. G., ter Heijne, A., Hamelers, H. V. M., & Buisman, C. J. N. (2018). (Bio)electrochemical ammonia recovery: progress and perspectives. In *Applied Microbiology and Biotechnology* (Vol. 102, Issue 9). <https://doi.org/10.1007/s00253-018-8888-6>
- Li, Y., Shi, S., Cao, H., Wu, X., Zhao, Z., & Wang, L. (2016). Bipolar membrane electrodialysis for generation of hydrochloric acid and ammonia from simulated ammonium chloride wastewater. *Water Research*, 89. <https://doi.org/10.1016/j.watres.2015.11.038>
- Mehdizadeh, S., Yasukawa, M., Abo, T., Kakihana, Y., & Higa, M. (2019). Effect of spacer geometry on membrane and solution compartment resistances in reverse electrodialysis. *Journal of Membrane Science*, 572, 271–280. <https://doi.org/10.1016/j.memsci.2018.09.051>
- Mehta, C. M., Khunjar, W. O., Nguyen, V., Tait, S., & Batstone, D. J. (2015). Technologies to recover nutrients from waste streams: A critical review. In *Critical Reviews in Environmental Science and Technology* (Vol. 45, Issue 4). <https://doi.org/10.1080/10643389.2013.866621>
- Pashkevich, M. A., Alekseenko, A. V., & Petrova, T. A. (2019). Application of polymeric materials for abating the environmental impact of mine wastes. *Journal of Physics: Conference Series*, 1384(1). <https://doi.org/10.1088/1742-6596/1384/1/012039>
- Post, J. W., Hamelers, H. V. M., & Buisman, C. J. N. (2008). Energy recovery from controlled mixing salt and fresh water with a reverse electrodialysis system. *Environmental Science and Technology*, 42(15). <https://doi.org/10.1021/es8004317>
- Shi, L., Hu, Y., Xie, S., Wu, G., Hu, Z., & Zhan, X. (2018). Recovery of nutrients and volatile fatty acids from pig manure hydrolysate using two-stage bipolar membrane electrodialysis. *Chemical Engineering Journal*, 334. <https://doi.org/10.1016/j.cej.2017.10.010>
- Siddiqui, A., Lehmann, S., Haaksman, V., Ogier, J., Schellenberg, C., van Loosdrecht, M. C. M., Kruithof, J. C., & Vrouwenvelder, J. S. (2017). Porosity of spacer-filled channels in spiral-wound membrane systems: Quantification methods and impact on hydraulic characterization. *Water Research*, 119. <https://doi.org/10.1016/j.watres.2017.04.034>
- van Linden, N., Bandinu, G. L., Vermaas, D. A., Spanjers, H., & van Lier, J. B. (2020). Bipolar membrane electrodialysis for energetically competitive ammonium removal and dissolved ammonia production. *Journal of Cleaner Production*, 259. <https://doi.org/10.1016/j.jclepro.2020.120788>
- Vermaas, D. A., Saakes, M., & Nijmeijer, K. (2014). Enhanced mixing in the diffusive boundary layer for energy generation in reverse electrodialysis. *Journal of Membrane Science*, 453. <https://doi.org/10.1016/j.memsci.2013.11.005>
- Wikipedia contributors. (2023, September 2). Silicon. In *Wikipedia, The Free Encyclopedia*. Retrieved 08:55, September 5, 2023, from <https://en.wikipedia.org/w/index.php?title=Silicon&oldid=1173410593>

Wikipedia contributors. (2023, August 23). Polyethylene terephthalate. In *Wikipedia, The Free Encyclopedia*. Retrieved 09:00, September 5, 2023, from https://en.wikipedia.org/w/index.php?title=Polyethylene_terephthalate&oldid=1171919540

Xie, M., Shon, H. K., Gray, S. R., & Elimelech, M. (2016). Membrane-based processes for wastewater nutrient recovery: Technology, challenges, and future direction. In *Water Research* (Vol. 89). <https://doi.org/10.1016/j.watres.2015.11.045>

Zheng, Y., Jin, Y., Zhang, N., Wang, D., Yang, Y., Zhang, M., Wang, G., Lee, S., & Qu, W. (2022). Recovery of N, N-dimethylglycine (DMG) from dimethylglycine hydrochloride by bipolar membrane electrodialysis. *Chemical Engineering and Processing - Process Intensification*, 176. <https://doi.org/10.1016/j.cep.2022.108943>

6. Supplementary Index:

SI.1 Experimental Set-up



Fig. 1.1: Borosilicate solution bottles

These are the borosilicate bottles of each compartment naming, diluate (1 liter bottle), acid, base, and ERS (500 ml bottles). These are stirred on a mixing plate with the help of magnetic stirrers. The image also shows IDS SenTix 940 pH meters and TetraCon 925 EC meters.



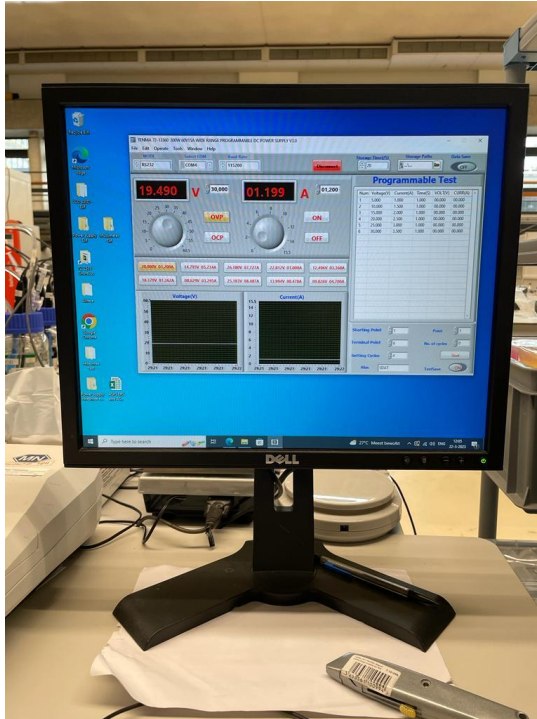
Fig. 1.2: Pump with pump heads of each compartment

Here, we see the Peristaltic Watson-Marlow 520S pump with separate 4 Watson-Marlow 313 pump heads for diluate, acid, base and ERS.



The electric current and potential were applied using a TENMA 72-1330 power supply box.

Fig. 1.3: Pump with pump heads of each compartment



This is the software in the computer through which we can adjust the power supply in the power supply box and can store data on the required path.

Fig. 1.4: Software for storing the power data

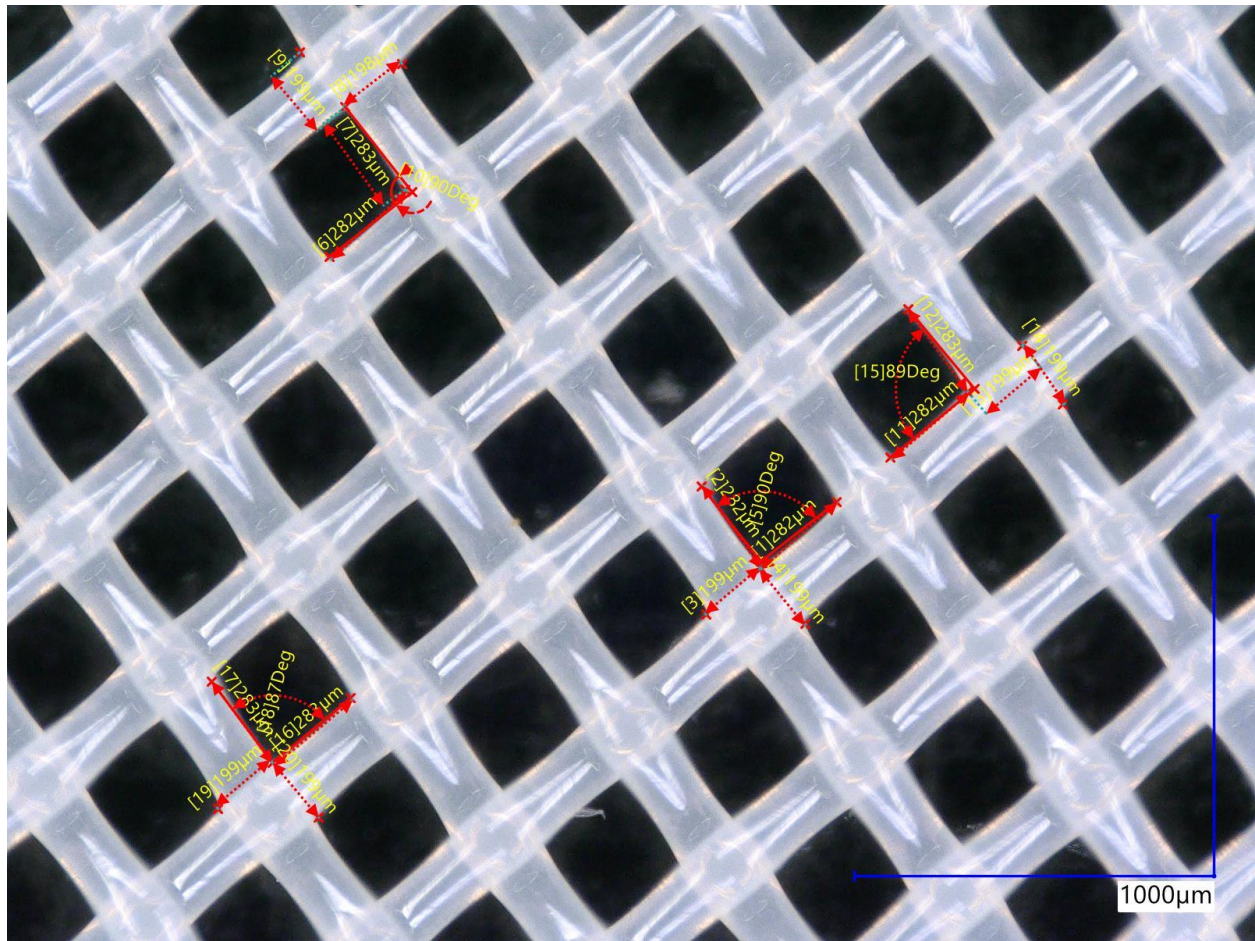


For pH, WTW Multi 3620 IDS multimeters, and for EC, WTW Multi 3620 IDS multimeters.

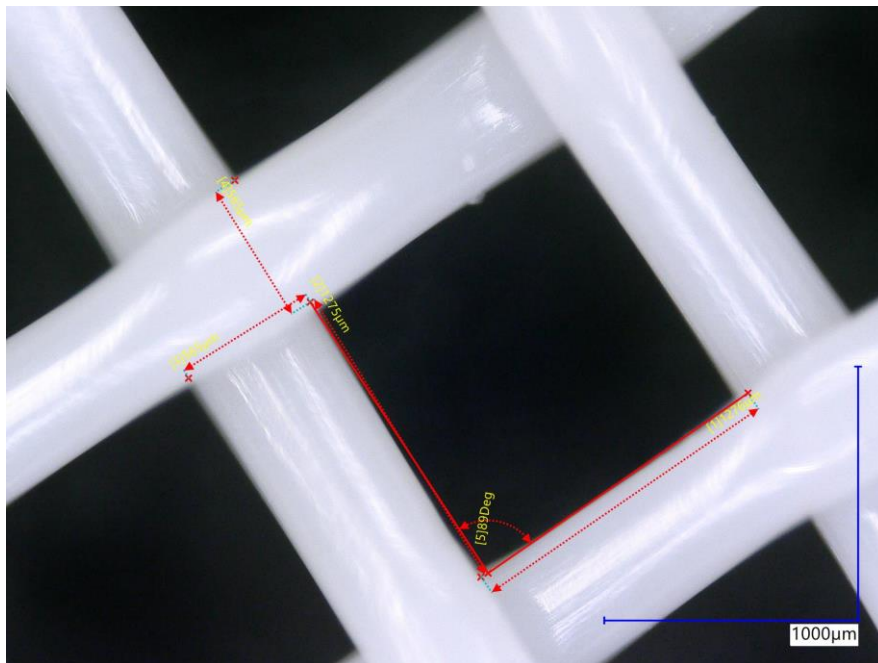
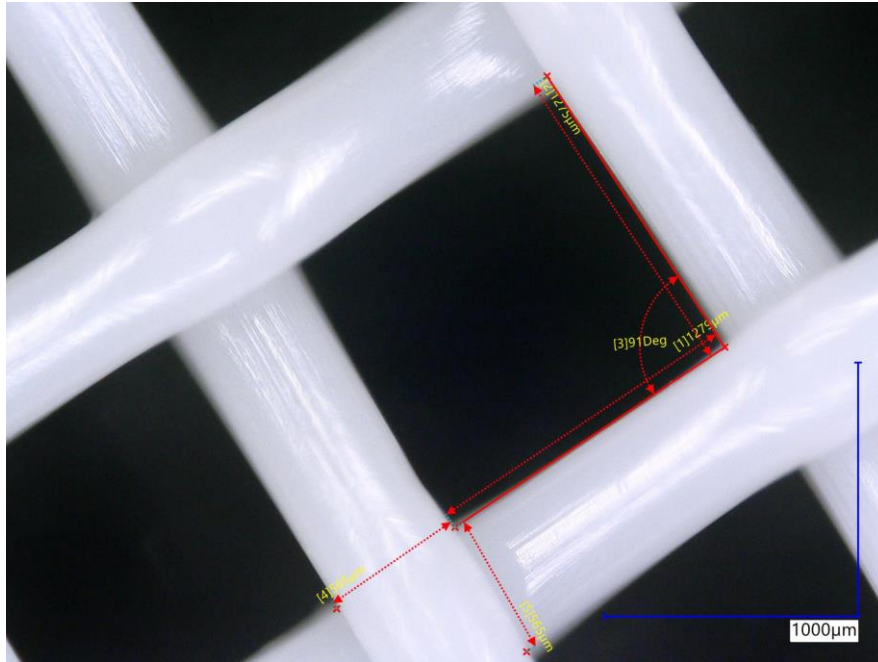
Fig. 1.5: Multimeters to record to pH and EC data

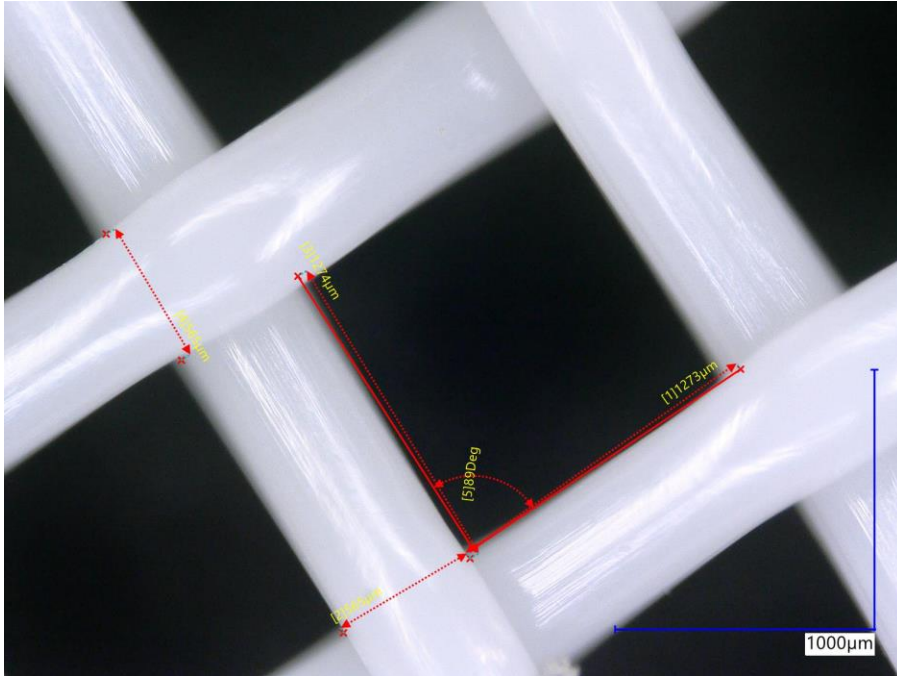
SI.2 Microscopic views of different spacers (with different thickness) along with measurements

SI.2.1 140 μm thick spacer:

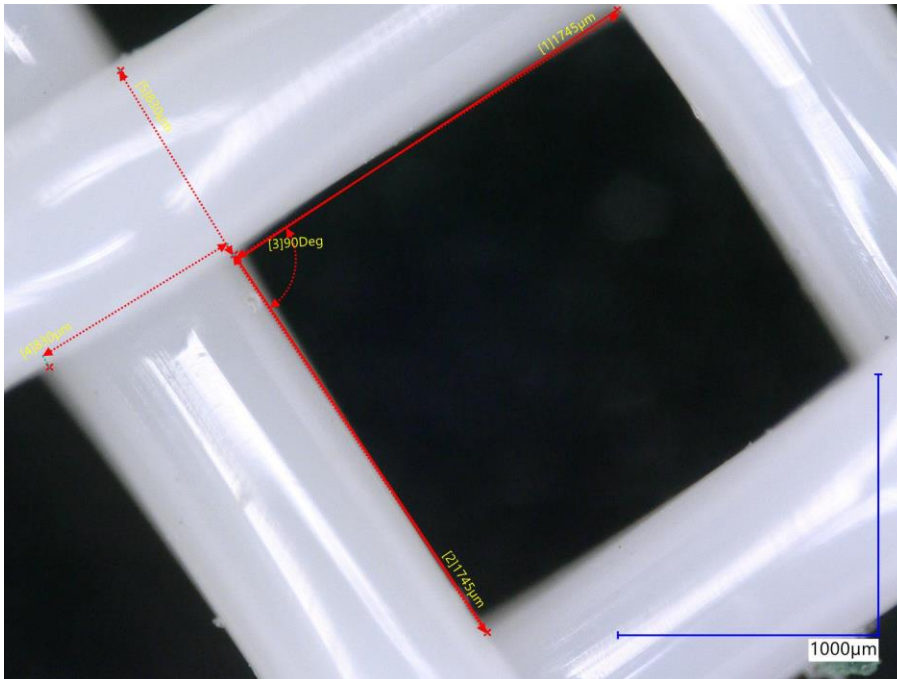


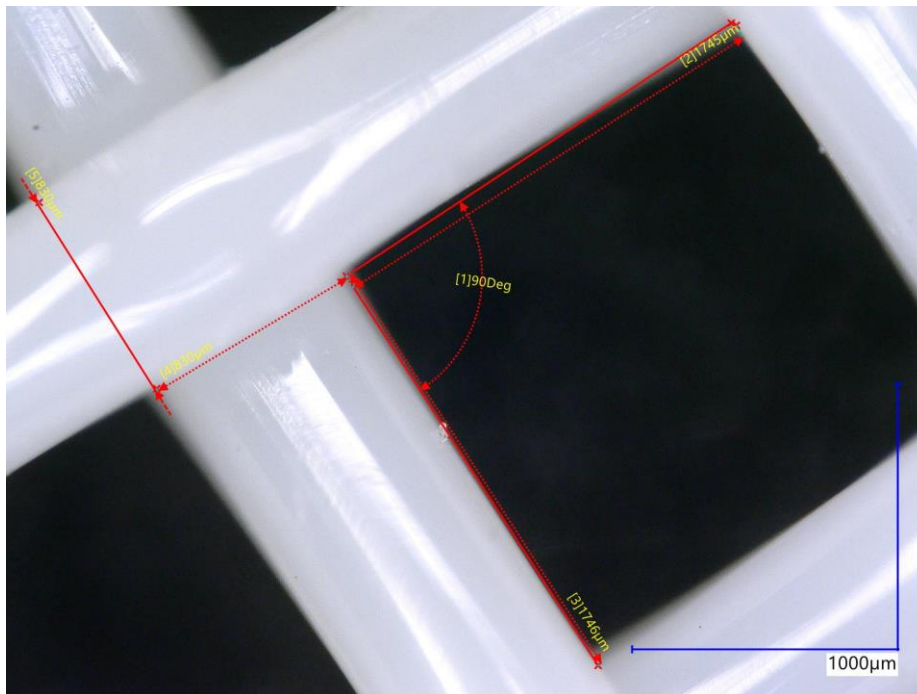
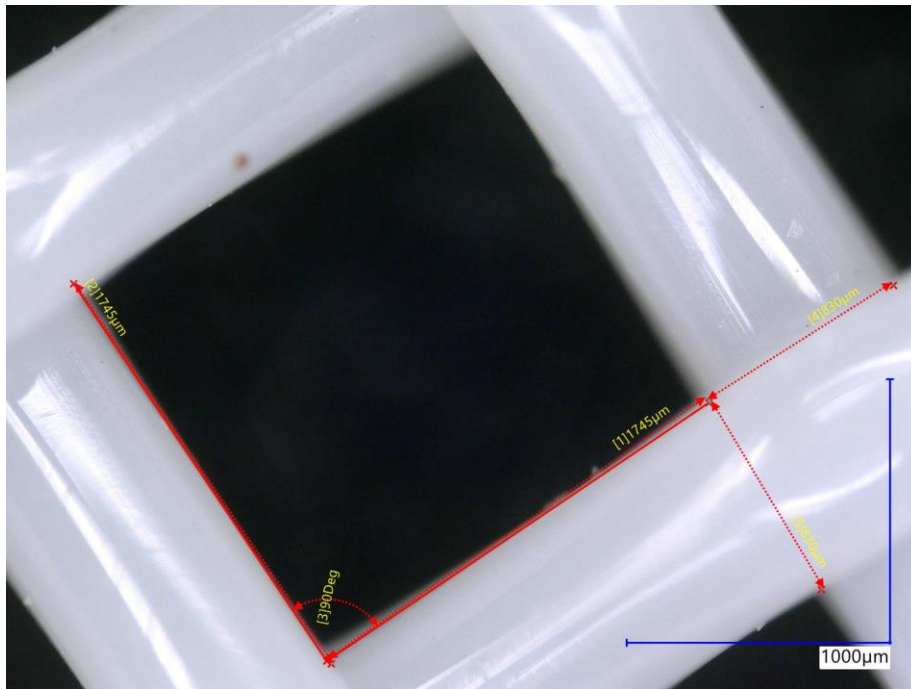
SI.2.2 450 μm thick spacer:





SI.2.3 750 µm thick spacer:





SI.3 pH and EC graphs for all the compartments

SI.3.1 Diluate

pH:

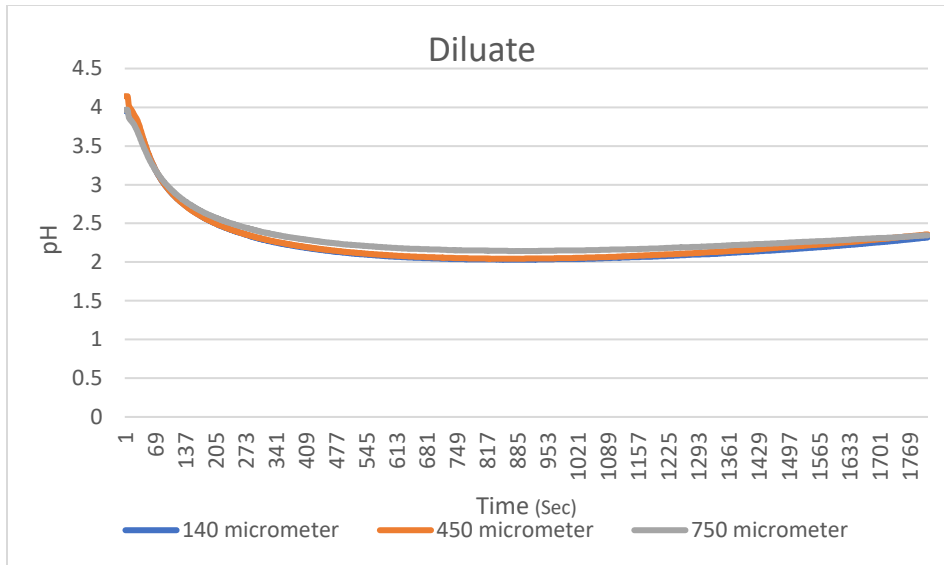


Fig. 3.1.1: Comparative pH graph of diluate of three spacers throughout the batch

EC:

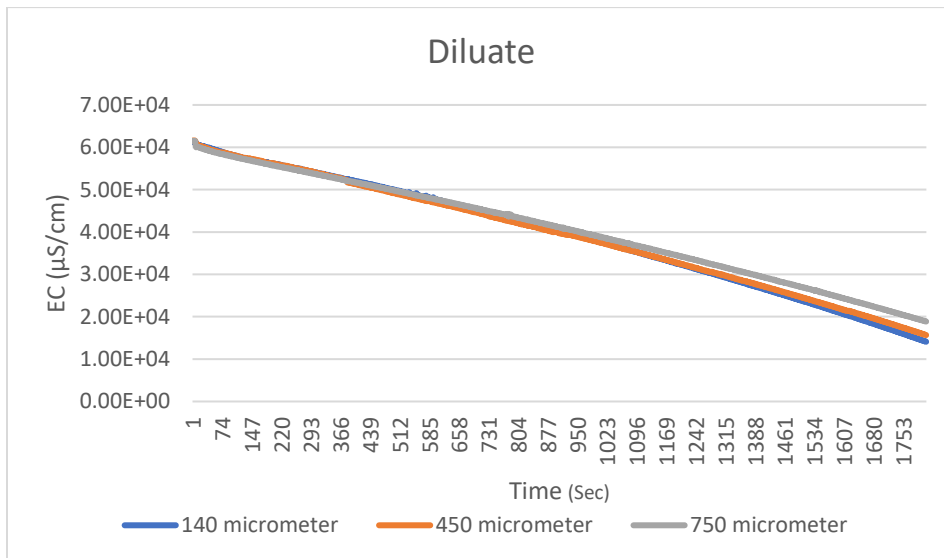


Fig. 3.1.2: Comparative EC graph of diluate of three spacers throughout the batch

SI.3.2 Base

pH:

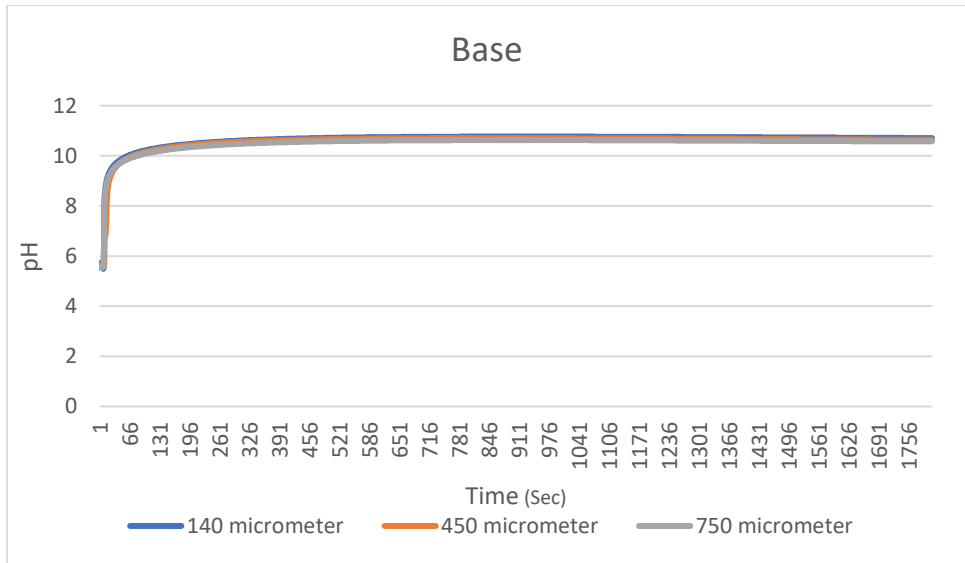


Fig. 3.2.1: Comparative pH graph of base of three spacers throughout the batch

EC:

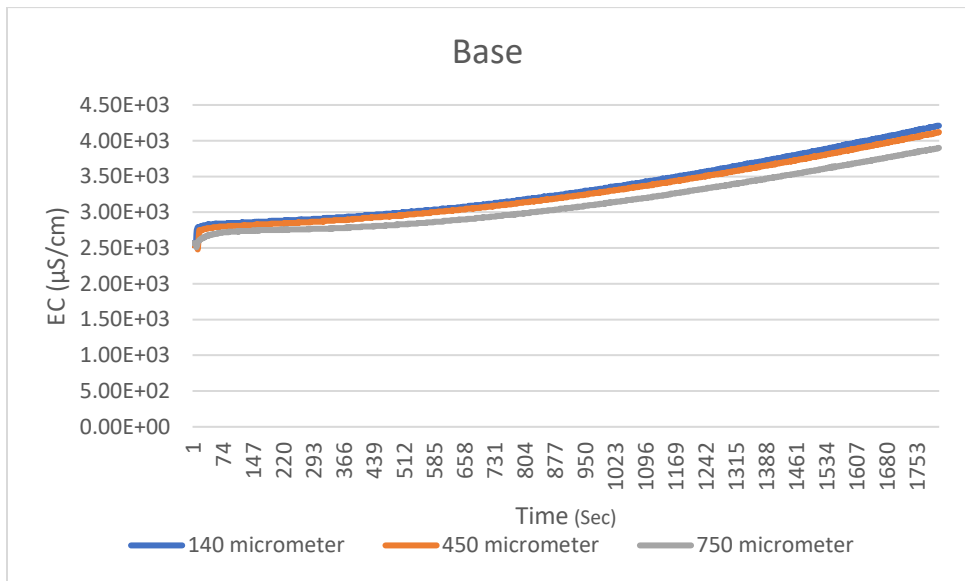


Fig. 3.2.2: Comparative EC graph of base of three spacers throughout the batch

SI.3.3 Acid

pH:

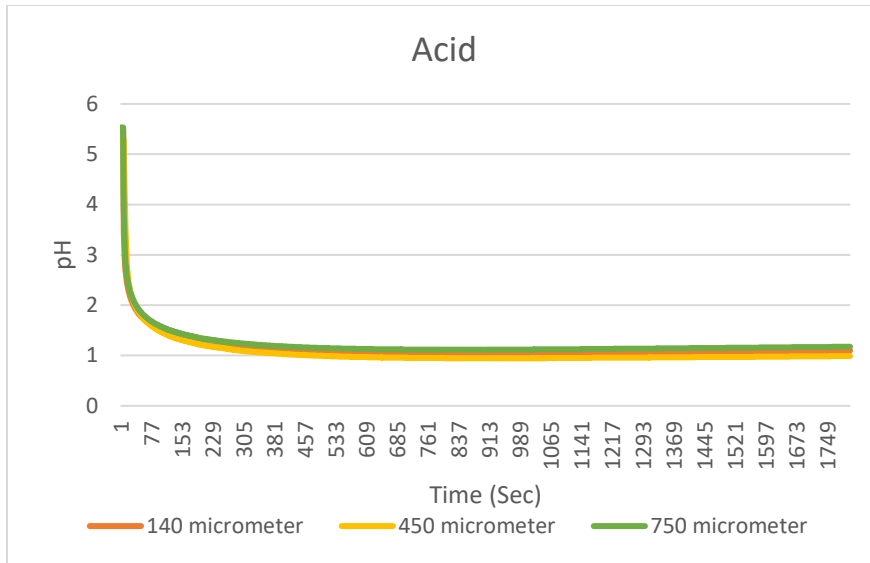


Fig. 3.3.1: Comparative pH graph of acid of three spacers throughout the batch

EC:

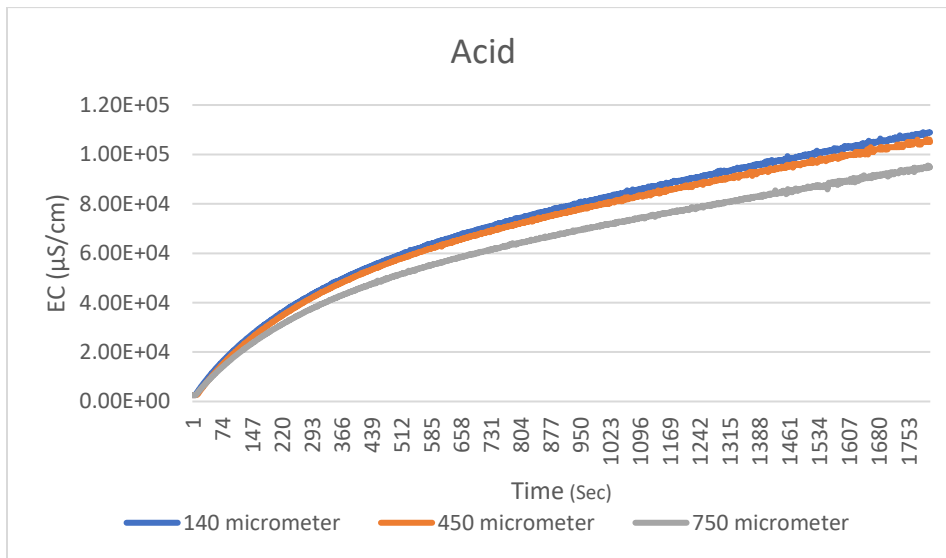


Fig. 3.3.2: Comparative EC graph of acid of three spacers throughout the batch

SI.4 Values and graphs of ammonium and sulfate concentrations throughout the batch

SI.4.1 Ammonium conc.:

140 micrometer (ppm)			
Time	Diluate	Acid	Base
0	13485.75	355.27	359.443
75	7026.8667	5182.3667	9590.9
150	2059.541667	12164.4667	10617.2667

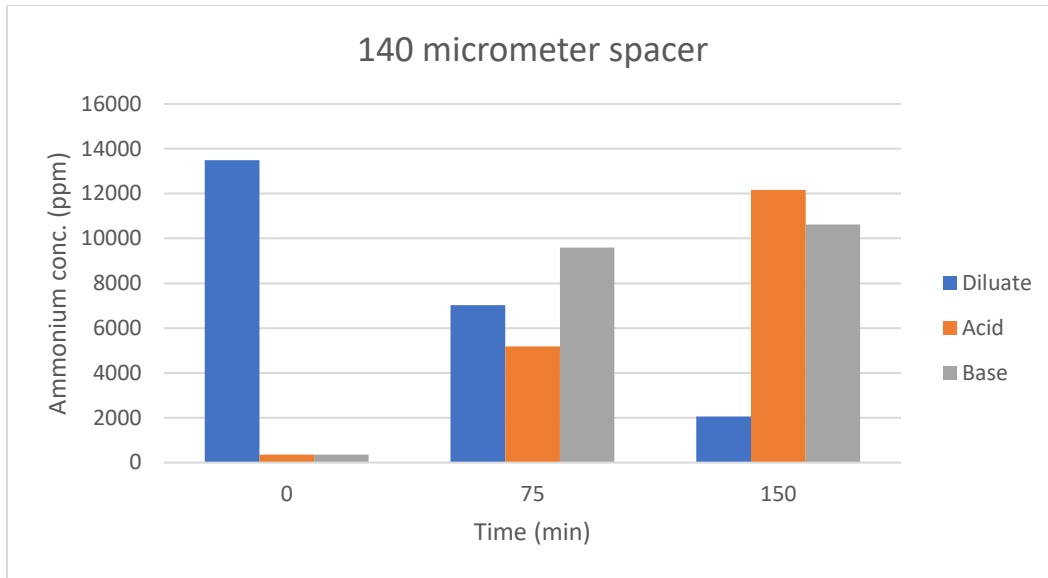


Fig.4.1.1: Graphical representation of ammonium transportation from diluate into acid and base using 140 μm thick spacer throughout the batch

450 micrometer (ppm)			
Time	Diluate	Acid	Base
0	12981.625	361.43	348.45667
75	7040.2667	4890.5333	7912.1833
150	2402.5833	11228.4	9024.31667

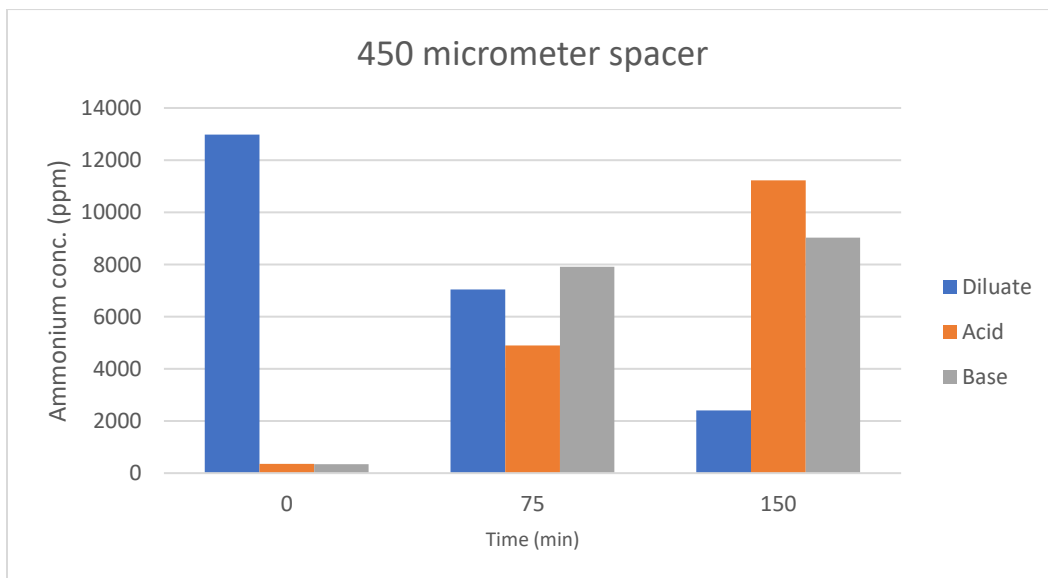


Fig.4.1.2: Graphical representation of ammonium transportation from diluate into acid and base using 450 μm thick spacer throughout the batch

750 micrometer (ppm)			
Time	Diluate	Acid	Base
0	13478.125	374.7333	371.75667
75	7606.8667	4832.9667	5694.9833
150	3069.6667	11522.8	6617.45

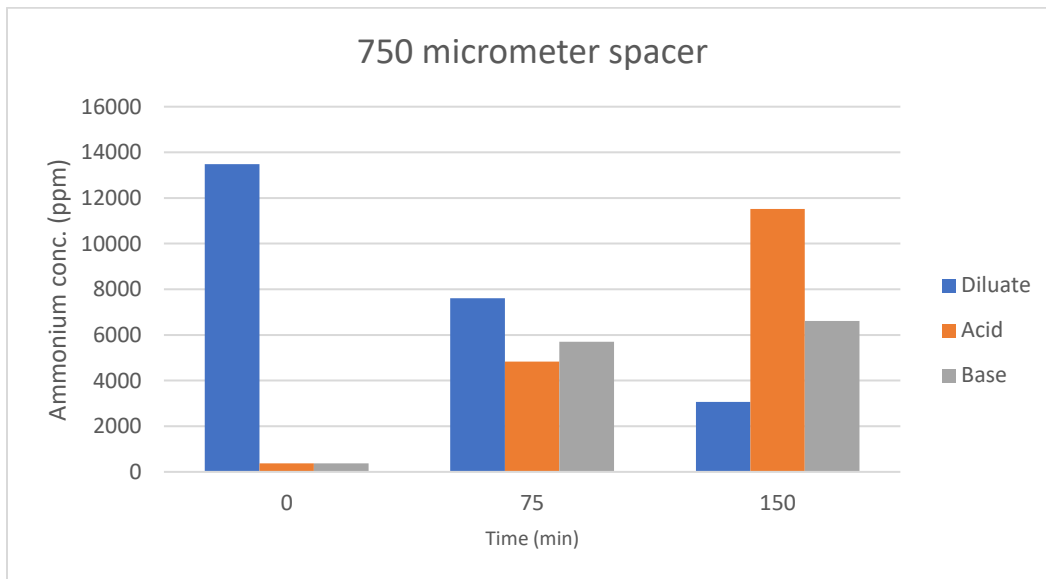


Fig.4.1.3: Graphical representation of ammonium transportation from diluate into acid and base using 750 μm thick spacer throughout the batch

SI.4.2 Sulfate Conc.:

140 micrometer (ppm)			
Time	Diluate	Acid	Base
0	35533.1667	948.88	943.65
75	20911.6667	29419.3	1053.6
150	6083.6	52463.8	1450.51667

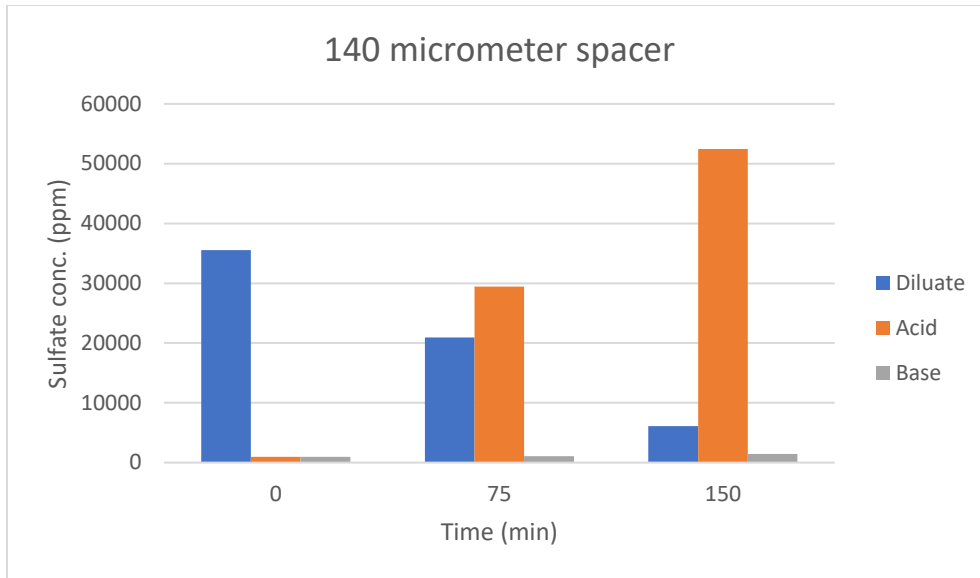


Fig.4.2.1: Graphical representation of sulfate transportation from diluate into acid and base using 140 μm thick spacer throughout the batch

450 micrometer (ppm)			
Time	Diluate	Acid	Base
0	36371.20833	926.2233	897.9433
75	21293.133	28451.9667	1035.5
150	7291.646	49733.2	1380.533

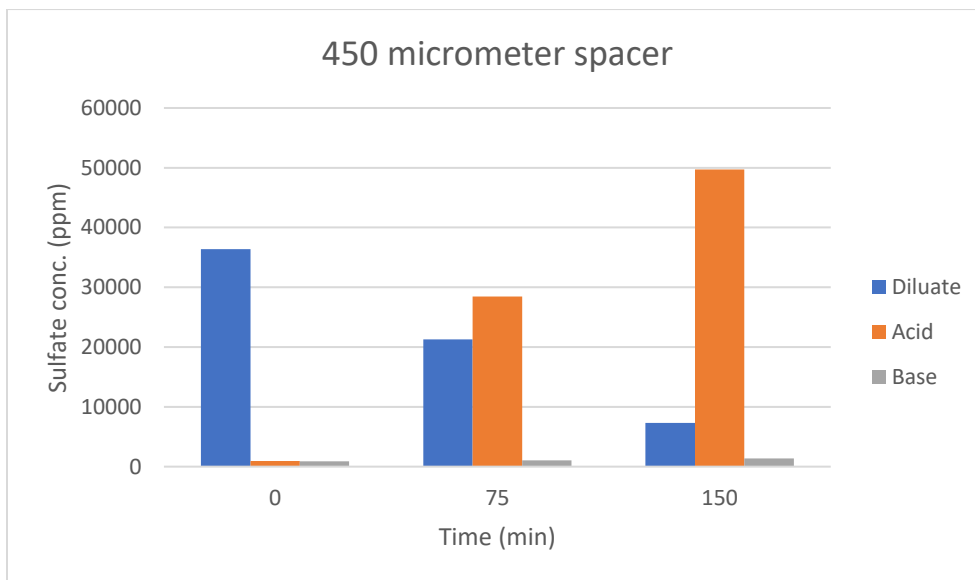


Fig.4.2.2: Graphical representation of sulfate transportation from diluate into acid and base using 450 μm thick spacer throughout the batch

750 micrometer (ppm)			
Time	Diluate	Acid	Base
0	35037.75	898	896.85
75	21129.433	25741	1024.3667
150	8500.75	46006.933	1342.3667

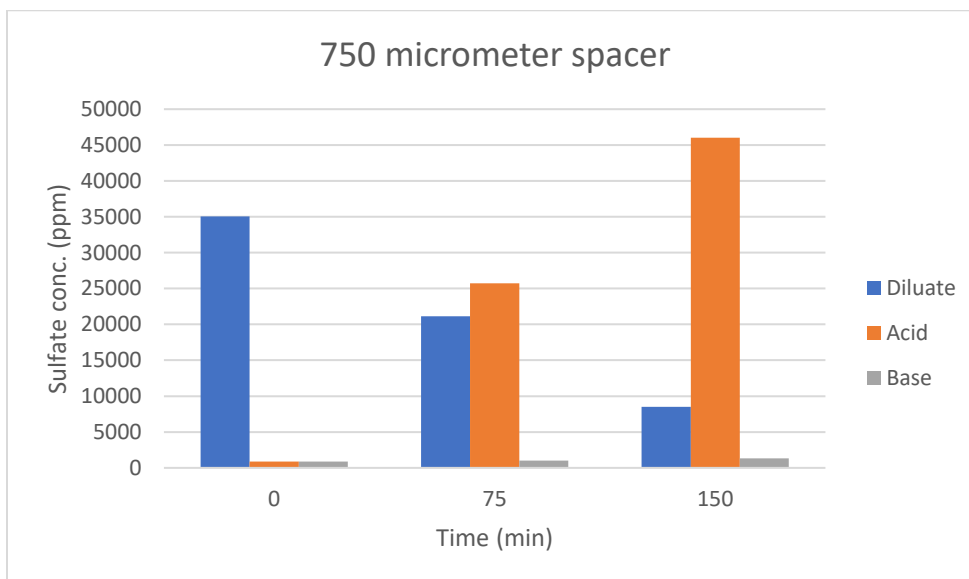


Fig.4.2.3: Graphical representation of sulfate transportation from diluate into acid and base using 750 μm thick spacer throughout the batch

SI.5 Computation of average electrochemical energies for other data

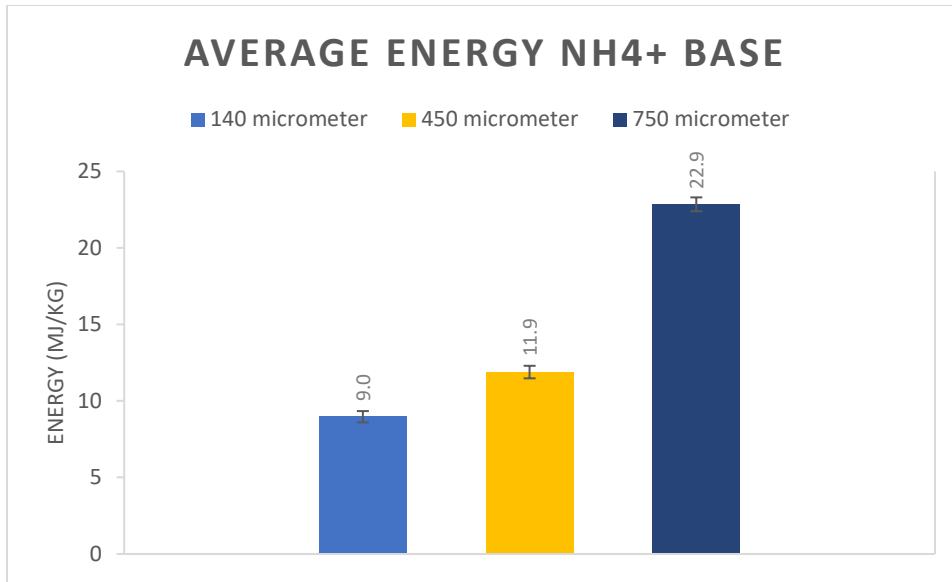


Fig. 5.1: Average energy consumption to transport ammonium in base

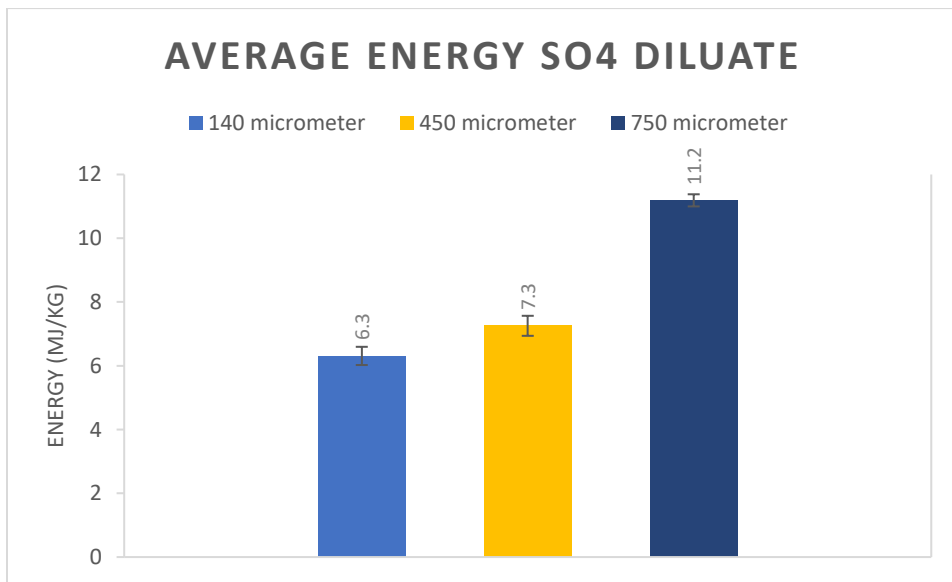


Fig. 5.2: Average energy consumption to transport sulfate from diluate

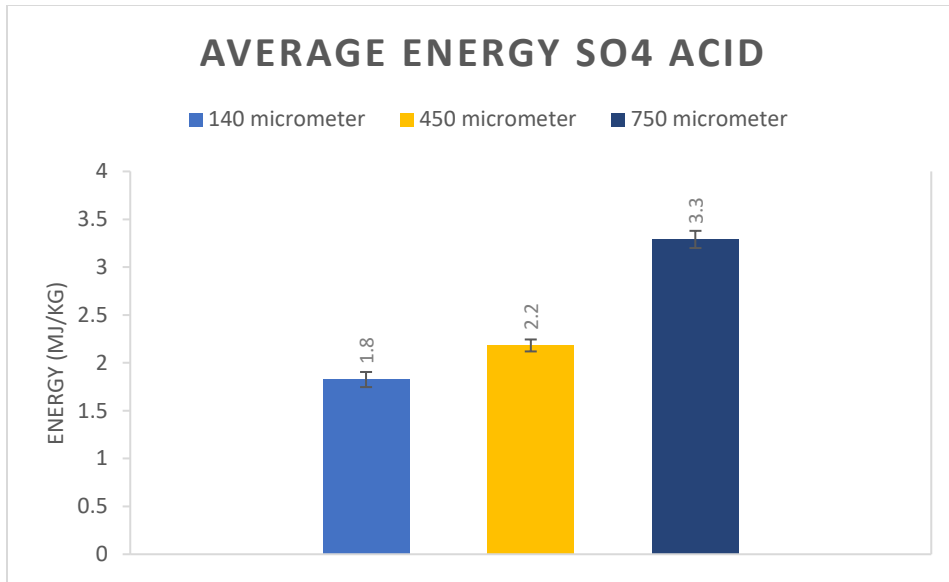


Fig. 5.3: Average energy consumption to transport sulfate in acid